Progress In Electromagnetics Research M, Vol. 25, 255–268, 2012

SELF-COLLIMATION EFFECT IN TWO-DIMENSIONAL PHOTONIC CRYSTAL BASED ON OPTOFLUDIC TECHNOLOGY

M. Ebnali-Heidari[1, *], F. Forootan[1], and A. Ebnali-Heidari[2]

[1]Faculty of Engineering, University of Shahrekord, Shahrekord 8818-634141, Iran

[2]Physics Department, University of Isfahan, Isfahan 81746, Iran

Abstract—We propose an optofluidic based on two-dimensional (2D) rod-type silicon photonic crystal (PhC) waveguide that supports self-collimation effect over a large frequency and angle range without any defect or nano-scale variation in the PhC geometry. By analyzing the equi-frequency counter (EFC) of a triangular rod PhC-bands, we verify the optimum band of the structure which is suitable for self-collimation of light beams. By varying the refractive index of fluid being infiltrated into the background of PhC, we perform a systematic study of optofluidic self-collimation of light beams to achieve a wide range of angles and low loss of light. By means of selective microfluidic infiltration and remarkable dispersion properties, we show that it is possible to design auto-collimatator and negative refraction devices based on self-collimation effect with high transmission. We use the plane wave method (PWM) for analyzing the EFC and the finite difference time domain (FDTD) method for simulating the transmission properties.

1. INTRODUCTION

Photonic crystals, first introduced by John [1] and Yablonovitch [2] in 1987, have natural advantages of controlling the propagation of light in the wavelength-scale. In recent years, there has been growing interest in using PhCs to design different telecommunication devices such as switch [3, 4], router [5], and all optical logic gates [6]. Most of the research works reported in designing of PhC devices are based on the photonic band gap (PBG) properties [7–9]. The devices based on this

Received 21 July 2012, Accepted 20 August 2012, Scheduled 5 September 2012

* Corresponding author: Majid Ebnali-Heidari (ma.ebnali@gmail.com).

method rely on the optimization of the PhC lattice geometry, where the high fabrication accuracy is essential, as even nanometre-scale deviations typically lead to a significant degradation in the desirable optical dispersion properties [10–13]. However, in recent years the devices based on self-collimation of light beams and negative refraction in PhC without geometry variation are proposed [14–18]. Self-collimation (SC) effect, by which an incident light can propagate with almost no diffraction and no engineered defect in PhCs, has attracted particular attention because of its potential for photonic integrated circuit (PIC) [19, 20]. Self-collimation is independent of light intensity, nonlinear propagation and frequency ranges. Moreover compared with engineered defect PhCs waveguides, self-collimation doesn't required lateral confinement to prevent either the beam divergence or diffraction broadening and it can release strict alignment for coupling light into narrow waveguide. To use these effects in practical device, it is essential that light can be coupled efficiently into and out of the PhC structure with minimal back-reflection. The self-collimation effect relies on the special dispersion properties in PhC, where the curvature of equi-frequency counter (EFC) departed from the normally circular curvature in free space. This property is achieved when this curvature becomes flat [21–23]. Also this curvature has the ability to generate the negative refractive index. In this paper, we propose a two-dimensional (2D) triangular rod-type photonic crystal lattice waveguide that support self-collimation effect over a large frequency and angle range using the optofluidic approach. Optofluidics is a new branch of photonics and microfluidics [26, 27]. In particular, combination of PhC structures and microfluids has attracted some attention as a means to tune the optical properties of PhC [28, 29], which means that background fluid infiltration offers free parameter which is independent of the fabrication. However, the most important aspect of microfluidic is the potential for reconfigurable properties which could overcome these topological limitations [30, 31].

In this paper, we show the optimization process of light coupling and transmission in the SC region by injecting fluids with various refractive indexes to background of photonic crystal rods. We also show that the self-collimated beams can be easily controlled by varying the refractive indexes of infiltrated fluid. In order to analyze the EFC calculations, we have performed the plane wave method (PWM). Then by employing the finite different time domain (FDTD) method with perfectly matched layer boundary condition, the transmission properties of rod-type photonic crystals have been studied.

The rest of this paper is organized as follow. In Section 2, we review the theoretical foundations of self-collimation phenomenon and its corresponding EFC map. After that, the suitable structure, by analyzing and calculating different parameters, is achieved. The procedure to optimize and reconfigure self-collimation and negative refraction properties by means of selective optofluidic background infiltration through precision simulation techniques is presented in Section 3. Finally, we conclude the paper in Section 4.

2. STRUCTURE DESIGN AND ANALYSIS

2.1. Self-collimation Effect in Photonic Crystal Structures

Photonic crystal structures provide the mechanism to control and confine the light. The existence of a bandgap in PhC helps the majority of applications to confine light in space. However, by exciting the modes of photonic crystal with frequencies outside the photonic bandgap, light can propagate in the PhC. Then, due to the complex spatial dispersion properties of planar photonic crystals, phenomena associated with anomalous refraction of light such as a super-prism or self-collimation can occur. Self-collimation or self guiding of light in a perfectly periodic photonic crystal is a process, in which a narrow beam of electromagnetic wave can propagate without any significant broadening or diverging in beam profile. It has been demonstrated that PhCs applications based on self-collimation effects rely on in-band properties rather than bandgap. In this application, the property of guiding mechanism relies on the shape of band, rather than bandgap. The PWM is used to calculate the band structure. In our simulation because the proposed SC PhC waveguide has no defect, we employed a unit cell instead of complex supercell calculation for the lattice.

It is known that in an inhomogeneous medium such as photonic crystals, the light propagation can be controlled by the direction of its group velocity given by $v_g = \nabla_k \omega(k)$, which is perpendicular to the equi-frequency contour [15]. Also the SC effect is achieved when the equi-frequency contours are as flat as possible, because the group velocity of light is always normal to the equi-frequency contours.

Light coupling from a homogeneous dielectric medium to Bloch modes of PhC can be described in terms of conservation of momentum (wavevector) or by a generalised version of Snell's law. The schematic of this light coupling according to Snell's law is presented in Fig. 1(a). In this figure, θ_i and θ_{pc} represent the incident and transmitted light angles in a homogeneous dielectric and a PhC medium, respectively. Fig. 1(a) shows that when the plane wave passes from the air to the PhC, it bends according to Snell's law. The bending angle depends on refractive index of each medium. In order to find the frequency range

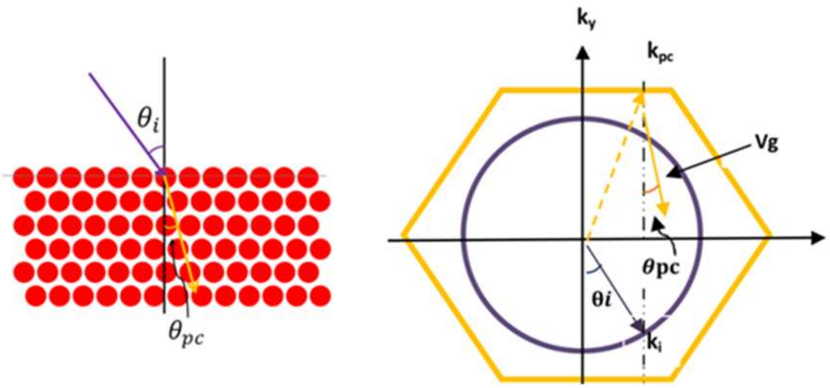

(a) (b)

Figure 1. (a) Geometry showing the creation of incident and transmitted light at the boundary of a homogenous dielectric and a PhC media according to snell law, (b) the equifrequency contour of two homogeneous isotropic dielectrics and a PhC.

in which the self-collimation effect takes place, the EFCs calculation, as a function of in-plane k vector, is essential.

A plane wave of frequency ω propagating in a homogeneous dielectric medium with refractive index n is characterized in space by a wavevector of magnitude $k = n\omega/c$ and its propagation direction. The set of all possible wavevectors at this frequency illustrated by a circle of radius k, as a result by considering various frequencies existence, leads to creation of different circles. These circles are EFCs of conical band surface related to homogeneous dielectric. As mentioned earlier, an EFC provides a valuable representation of light dispersion in any homogeneous or inhomogeneous media. The EFC for the homogeneous medium is circular. However, these circular curvatures change in inhomogeneous medium. For instance, in triangular PhC lattice, the circular curvature turns to nearly hexagonal EFC. In this case, the EFC of photonic crystals moves to the flat sides, where the self-collimation effect can occur. This can be described by the group velocity behaviour of k vector over broad ranges that cause the beams of light to collimate in such a PhC. The schematic of this behaviour is illustrated in Fig. 1(b). The purple circle and arrow indicate air medium EFC and incident wavevector, k_i, respectively, at the incident frequency. The yellow curve and dashed arrow are the EFC counter of PhC and refractive wavevector, k_{pc}, respectively, and the group velocity vector of refracted wave, v_g, is indicated by solid yellow arrow. It should be noted that in the self collimation of light beams, the group

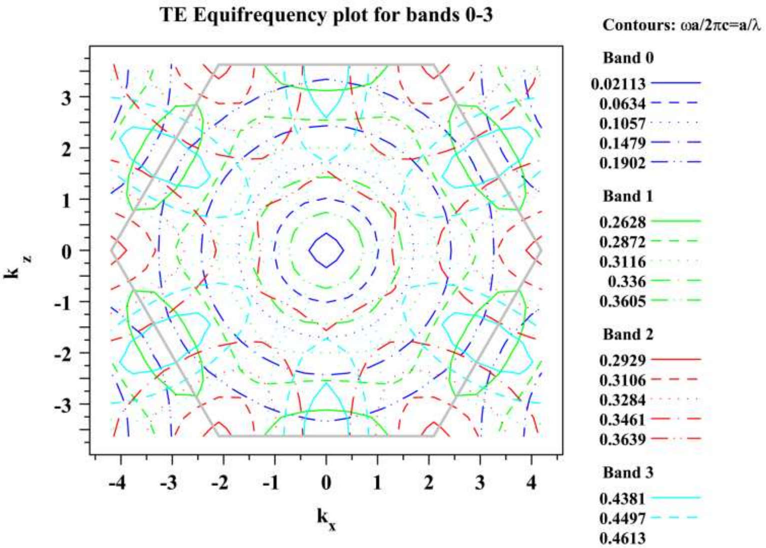

Figure 2. The EFC plot of four bands related to paper structure of a rod hexagonal PhC.

velocity and phase velocity have the same direction; meanwhile in the case of negative refraction, their directions become opposite. In this case, the phase velocity is opposite to the group velocity and happens at angular convex EFC map.

2.2. Structure Design

The basic structure of the proposed PhC waveguide has a triangular lattice with refractive index of 3.5 and 1 for silicon rods and background, respectively. We restrict our calculations to transverse-electric (TE) polarization states, i.e., with the magnetic field parallel to the rod axes. The EFC plot of the four bands with TE polarization states is presented in Fig. 2. The flat part of the EFC, which is perpendicular to the Γ–M direction, shows that the self-collimation phenomenon occurs along this direction if a TE polarized beam propagates in the PhC at a frequency of $a/\lambda = 0.28$, where a is lattice constant, and λ indicates incident light wavelength. Thus we choose the dashed green line in Fig. 3 to indicate this frequency, as the working frequency. The other reason for the second band selection is that the light coupling into the higher-order Brillion zones can sometimes occur for non-normal incidence and beam divergence. In order to optimize the transmission pattern, we examine different rod

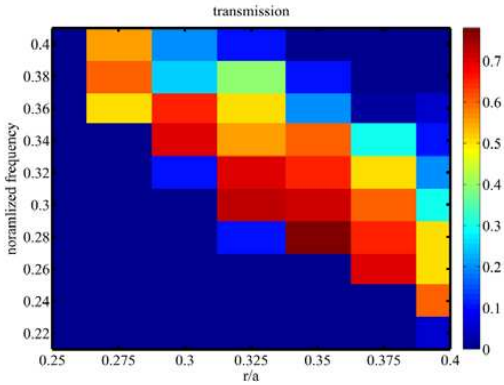

Figure 3. Transmittance contour plots for for Normalized frequency a/λ versus different ratio of r/a in rod-type hexagonal PhC for a fixed incident angle, $\theta_i = 0°$.

radii versus second band structure of hexagonal rod PhC lattice for $\theta_i = 0°$. The result is shown in Fig. 3. This figure shows that the highest transmission takes place in the rod radius range, from $0.34a$ to $0.36a$, for the normalized frequency of $a/\lambda = 0.28$ (second band) with TE polarization. Furthermore, this figure reveals that the value of optimized frequency decreases by increasing rod radius. According to Fig. 3, this structure shows the highest transmission for narrow band width. It means that there is limitation on working frequency range in self-collimation region. It is also difficult to obtain a large flat dispersion contour by a high symmetrical PhC. Some structures with less symmetric lattice geometries have been proposed in order to improve the performance of self-collimation. For broadening and tuning this band width range, it is possible to control or change the rods size during fabrication, but a complicated technological process is necessary. In this paper, we propose a remedy for these disadvantages by adopting a technique based on the background infiltration of the PhC lattice rather than careful nanometer-scale modification of the PhC geometry.

3. NUMERICAL SIMULATION OF OPTOFLUIDIC SC

3.1. Comparative Analysis of Self-collimation Transmission for Different Fluids and Frequencies

The simulation results, represented in Section 2, show that the conventional rod-type PhC with the air background (no fluid

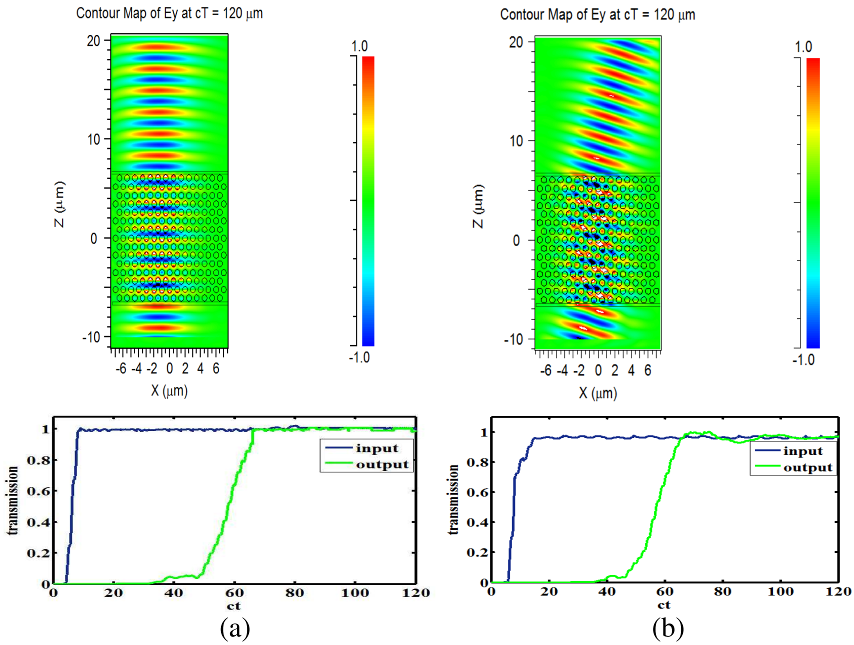

Figure 4. Self collimation simulation for TE polarization in rod hexagonal PhC with $n_f = 1.6$. Blue and green lines are transmission amplitude at input and output of phC waveguide receptively: (a) light coupling for incident light angle of $\theta_i = 0°$, (b) incident light angle of $\theta_i = 10°$ for negative refraction.

infiltration) and rod radius, $r = 0.35a$, is an optimum structure, due to the lowest back-reflectance. As a result, a reasonable self-collimation property belongs to the second band. Based on this structure, we examine the bandwidth tunability and transmission variation of lattice with fluid infiltration to optimize the device performance. To see the fluid infiltration effects, as an example for this paper, the self-collimation effect with high transmission pattern is achieved by optical fluid of refractive index $n_f = 1.6$ in the PhC background with $\theta_i = 0°$ in Fig. 4(a). By small increscent in incident light angle such as $\theta_i = 10°$ a different transmission pattern named negative refraction appears in Fig. 4(b). Temporal transmission diagram for TE polarization is shown by blue and green lines as input and output of phC waveguide receptively in the lower part of Fig. 4. Obviously, with no structural defect we have a complete transmission pattern for waveguiding in each pattern.

Negative refraction of electromagnetic (EM) waves is a phenomenon that light rays are refracted at an interface in the reverse sense to that normally expected. Before that, it was predicted that

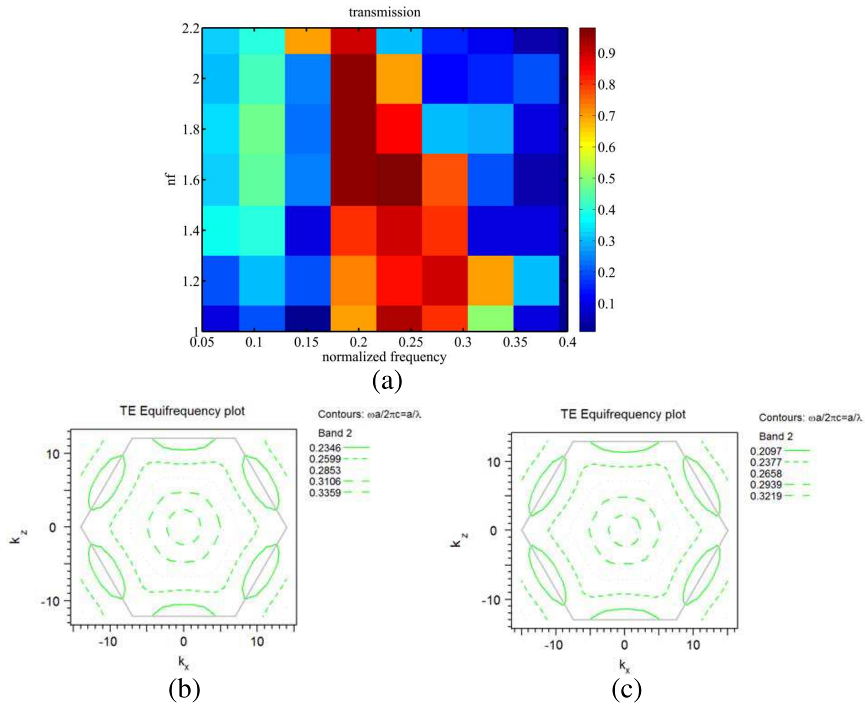

Figure 5. (a) Transmission color map for varying Normalized frequency a/λ and fluid refractive indices (n_f) in incident angle $\theta_i = 10^\circ$. EFCs plot: (b) $n_f = 1.4$, (c) $n_f = 1.6$.

negative refraction is characterized by simultaneous negative permittivity and permeability, but recently it has been achieved in photonic crystal with positive index to make super lenses with resolution far beyond the diffraction limit [24, 25]. Here we show the potential for generating negative refraction by using the optofluidic infiltration method. We have simulated light coupling with incident angle near $\theta_i = 10^\circ$ into bands, which have the desired dispersion properties. By focusing on above structure, the effect of the background fluid infiltration, on transmission for various fluids versus the normalized frequency, is shown in Fig. 5(a). The range of selected refractive indices of fluid, n_f, is chosen between 1.1 to 2.2. As shown in Fig. 5(a), by infiltrating the fluid with refractive index of 1.6, the large frequency range from 0.16 to $0.3(a/\lambda)$ with high transmission value (more than 85%) is obtained. It should be noted that in comparison with conversional PhC, uninfiltrated, large frequency range is enhanced nearly more than two times. Also the figure obviously shows the second band frequency changing by n_f conversion. Before Mendoza-Suarez et al. proposed the method to manipulate the band structure and gap width by just changing the phase difference or the amplitude of the surface profile in 1D PhC [32], however, the infiltration method is able to do the same work on EFC plot. To prove our claim, one can observe the frequency variation shown by straight dashed green lines in EFCs plot; according to selective fluid infiltration, Figs. 5(b) and (c) show the EFC plot as a sample for two arbitrary points, $n_f = 1.4$ and 1.6. The dashed green lines in EFC specify the best SC normalized frequency which is $a/\lambda = 0.258$ and $a/\lambda = 0.234$ for $n_f = 1.4$ and 1.6, respectively. It can be seen that when the fluid refractive index increases, the normalized frequency associated to counter map decreases. But the basic point is that we achieved both high transmission values (nearly 1) and large broadband width by injecting fluid refractive index from 1.3 to 1.9. While in conventional map with no infiltration (see Fig. 3), the maximum transmission for different rod radii was less than 0.8 and belongs to narrow bandwidth. Thus in the related frequencies range, the structure can be used as virtual waveguide with no channel and without introducing dielectric waveguide or line defects. Consequently, the beams of light can transport without scattering and broadening for TE polarization. And the structure also makes the effect of fluid on transmission values and tunability of PhC undeniable.

3.2. Comparative Analysis of Self Collimation and Negative Refraction Transmission Related to PhC Background Infiltration (n_f) Versus Different Incident Angles

When a plane wave is incident to the PhC structure with period a, the number of propagation modes depends on both normalized frequency (a/λ) and incident angle. In the previous section, we showed that

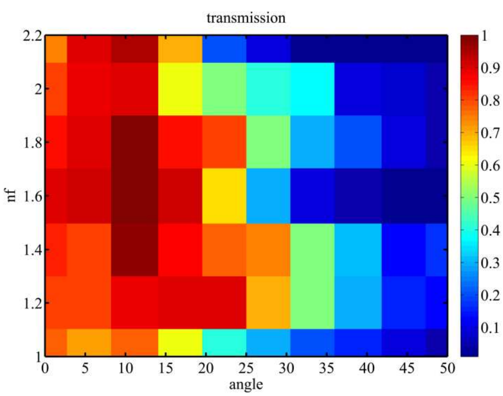

Figure 6. Transmittance contour plots for varying incident angles (θ_i) and fluid refractive indices (n_f).

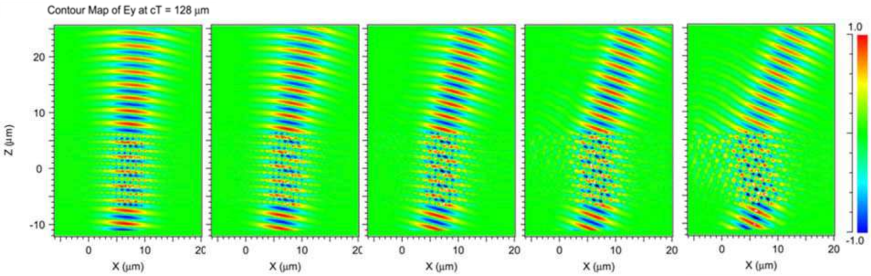

Figure 7. Negative refraction transmission pattern for different angles by selective infiltrated fluid with $n_f = 1.5$ and normalized frequencies, $f = 0.24a/\lambda$: (a) $\theta_i = 5°$, (b) $\theta_i = 10°$, (c) $\theta_i = 15°$, (d) $\theta_i = 20°$, (e) $\theta_i = 25^{\circ}$.

the SC effect for only a single angle $\theta_i = 10°$ related to negative refraction. However, as mentioned earlier, by fluid infiltration of the structure, the normalized frequency will be changed. In this case, we developed the method for different angles and fluids. However, it must be noted that the optimum SC frequency for the best transmission varied by different values of n_f, but in each situation, the EFC plot helped us to find the related frequency value. Here all the simulation result illustrated in Fig. 6, in which x axis is used for different incident angles from $\theta_i = 0°$ to $\theta_i = 50°$ and y axis refers to selective fluids. As can be seen, by simply changing the background refractive index of fluid from 1.3 to 1.7, the complete transmission for incident angles between $\theta_i = 0°$ to $\theta_i = 50°$ is achieved. The numerical results presented here, so far, show that the approach based on the selective optofluidic infiltration method is very robust, and the problem with fabrication inaccuracies can be compensated by using a different fluid index. As a result beside system tenability, many of the properties for lower refractive index contrast cause a larger range of materials available for fabrication. Furthermore, in Fig. 6 in which the incident angle increases, and yet the transmission value is high (angles nearly between 10° to 30°), we have negative refraction phenomenon in normal structure with no negative index martial, which is suitable for perfect super lens. But for θ_i more than 30°, most of the coupled light is reflected back. As a result, the reasonable collimation regime in PhC is accessible by reconfigurable technique of infiltration for angles less than $\theta_i = 25°$. Fig. 7 depicts transmission pattern related to $n_f = 1.5$ for different angles caucusing negative refraction. In this manner in spite of beam angle enhancement, light coupling and guiding in the lattice have a convincing performance, without any dispersion or broadening in beam profile. Also it is apparent from Fig. 7 that bending value of the output beam intensively depends on incident light angle. This relaxes the limitation on PhCs fabrication as compared to previous structural method such as waveguides defects or rods movement and leads us to realization of integrated circuits. However, an important technological constraint related to optofluidics is the accuracy of the infiltration method itself. A variety of selective infiltration techniques of planar PhC structures have been experimentally demonstrated using for instance an integrated microfluidic circuit [33], an actuated microtip [34] or micropipette [35] whose size is comparable to the PhC lattice. Also the background regions could be infiltrated with a high precision and good reproducibility. In addition, providing stable fluid of various n_f that has high tolerance in a different environmental temperature is undeniable challenge in optofludic approach.

4. CONCLUSION

In this paper, the effect of a new technique based on selective background liquid infiltration on novel selfcollimation phenomenon of 2D rod hexagonal lattice is discussed. The proposed structure acts as a virtual waveguide with no defect that can propagate light with no serious diffraction or broadening. The simulation result shows that by controlling refractive index of the fluids into the background of rod-type planar PhC it creates a refractive index difference, which can lead us to making reconfigurable PhC self-collimation device with high transmission. For instance, the high transmission (nearly equal to 1) can be achieved by infiltration fluid with refractive index from 1.4 to 1.6. The results also show that the EFC and SC frequency is affected notably by changing the background refractive index of infiltrated fluids. In addition to SC waveguides, for particular incident angles, the structure exhibits negative refraction over long propagation length without any dispersion or broadening in beam pattern with high transmission. This optimization approach, infiltration-based approach, offers an additional and free parameter (which is independent of the fabrication) for achieving a desired SC and negative refraction effect in the PhC of integrated optical circuits.

ACKNOWLEDGMENT

The first author wishes to thank the University of Shahrekord for financial support.

REFERENCES

1. John, S., "Strong localization of photons in certain dielectric superlattices," *Phys. Rev. Lett.*, Vol. 58, 2486, 1987.
2. Yablonovitch, E., "Inhibited spontaneous emission in solid-state physics and electronics," *Phys. Rev. Lett.*, Vol. 58, No. 20, 2059–2062, 1987.
3. Li, J., J. He, and Z. Hong, "Terahertz wave switch based on silicon photonic crystals," *Applied Optics*, Vol. 46, 5034–5037, 2007.
4. Li, Z., Y. Zhang, and B. Li, "Terahertz photonic crystal switch in silicon based on self-imaging principle," *Optics Express*, Vol. 14, 3887–3892, 2006.
5. Almeida, V. R., C. A. Barrios, R. R. Panepucci, and M. Lipson, "All-optical control of light on a silicon chip," *Nature*, Vol. 431, 1081–1084, 2004.
6. Zhang, Y. and B. Li, "Optical switches and logic gates based on self-collimated beams in two-dimensional photonic crystals," *Optics Express*, Vol. 15, 9287–9292, 2007.
7. Notomi, M., "Theory of light propagation in strongly modulated photonic crystals: Refractionlike behavior in the vicinity of the photonic band gap," *Phys. Rev. B*, Vol. 62, 10696, 2000.
8. Johnson, S. G. and J. D. Joannopoulos, *Photonic Crystals: The Road from Theory to Practice*, Springer, 2002.
9. Kokabi, A., H. Zandi, S. Khorasani, and M. Fardmanesh, "Precision photonic band structure calculation of Abrikosov periodic lattice in type-II superconductors," *Physica C: Superconductivity*, Vol. 460, 1222–1223, 2007.
10. Mekis, A. and J. Joannopoulos, "Tapered couplers for efficient interfacing between dielectric and photonic crystal waveguides," *Journal of Lightwave Technology*, Vol. 19, 861, 2001.
11. Kuang, W., C. Kim, A. Stapleton, and J. D. O'Brien, "Grating-assisted coupling of optical fibers and photonic crystal waveguides," *Optics Letters*, Vol. 27, 1604–1606, 2002.
12. Talneau, A., P. Lalanne, M. Agio, and C. Soukoulis, "Low-reflection photonic-crystal taper for efficient coupling between guide sections of arbitrary widths," *Optics Letters*, Vol. 27, 1522–1524, 2002.
13. Säynätjoki, A., M. Mulot, J. Ahopelto, and H. Lipsanen, "Dispersion engineering of photonic crystal waveguides with ring-shaped holes," *Optics Express*, Vol. 15, 8323–8328, 2007.
14. Kosaka, H., T. Kawashima, A. Tomita, M. Notomi, T. Tamamura,

T. Sato, and S. Kawakami, "Self-collimating phenomena in photonic crystals," *Applied Physics Letters*, Vol. 74, 1212, 1999.

15. Rakich, P. T., M. S. Dahlem, S. Tandon, M. S. MihaiIbanescu, G. S. Petrich, J. D. Joannopoulos, L. A. Kolodziejski, and E. Ippen, "Achieving centimetre-scale supercollimation in a large-area two-dimensional photonic crystal," *Nature Materials*, Vol. 5, 93–96, 2006.
16. Prather, D. W., S. Shi, J. Murakowski, G. J. Schneider, A. Sharkawy, C. Chen, B. L. Miao, and R. Martin, "Self-collimation in photonic crystal structures: A new paradigm for applications and device development," *Journal of Physics D: Applied Physics*, Vol. 40, 2635, 2007.
17. Djeffal, Z. E., H. Talleb, D. Lautru, and V. Fouad-Hanna, "Negative refractive index behavior through magneto-electric coupling in split ring resonators," *Progress In Electromagnetics Research Letters*, Vol. 22, 155–163, 2011.
18. Hsu, H.-T. and C.-J. Wu, "Design rules for a Fabry-Perot narrow band transmission filter containing a metamaterial negative-index defect," *Progress In Electromagnetics Research Letters*, Vol. 9, 101–107, 2009.
19. Witzens, J. and A. Scherer, "Efficient excitation of self-collimated beams and single Bloch modes in planar photonic crystals," *JOSA A*, Vol. 20, 935–940, 2003.
20. Witzens L., M. Mazilu, and T. F. Krauss, "Beam steering in planar-photonic crystals: From superprism to supercollimator," *Journal of Lightwave Technology*, Vol. 21, 561, 2003.
21. Pustai, D., S. Shi, C. Chen, A. Sharkawy, and D. Prather, "Analysis of splitters for self-collimated beams in planar photonic crystals," *Optics Express*, Vol. 12, 1823–1831, 2004.
22. Chen, C., A. Sharkawy, D. Pustai, S. Shi, and D. Prather, "Optimizing bending efficiency of self-collimated beams in non-channel planar photonic crystal waveguides," *Optics Express*, Vol. 11, 3153–3159, 2003.
23. Prather, D. W., S. Shi, J. Murakowski, G. J. Schneider, A. Sharkawy, C. Chen, B. L. Miao, and R. Martin, "Self-collimation in photonic crystal structures: A new paradigm for applications and device development," *Journal of Physics D: Applied Physics*, Vol. 40, 2635, 2007.
24. Parazzoli, C., R. Greegor, K. Li, B. Koltenbah, and M. Tanielian, "Experimental verification and simulation of negative index of refraction using Snell's law," *Phys. Rev. Lett.*, Vol. 90, 107401–107401, 2003.

25. Shelby, R., D. Smith, and S. Schultz, "Experimental verification of a negative index of refraction," *Science*, Vol. 292, 77–79, 2001.
26. Monat, C., P. Domachuk, and B. Eggleton,, "Integrated optofluidics: A new river of light," *Nature Photonics*, Vol. 1, 106–114, 2007.
27. Ebnali-Heidari, M., C. Grillet, C. Monat, and B. Eggleton, "Dispersion engineering of slow light photonic crystal waveguides using microfluidic infiltration," *Optics Express*, Vol. 17, 1628–1635, 2009.
28. Hosseinibalam, F., S. Hassanzadeh, A. Ebnali-Heidari, and C. Karnutsch, "Design of an optofluidic biosensor using the slow-light effect in photonic crystal structures," *Applied Optics*, Vol. 51, 568–576, 2012.
29. Bakhshi, S., M. K. Moravvej-Farshi, and M. Ebnali-Heidari, "Proposal for enhancing the transmission efficiency of photonic crystal 60° waveguide bends by means of optofluidic infiltration," *Applied Optics*, Vol. 50, 4048–4053, 2011.
30. Bitarafan, M., et al., "Proposal for postfabrication fine-tuning of three-port photonic crystal channel drop filters by means of optofluidic infiltration," *Applied Optics*, Vol. 50, 2622–2627, 2011.
31. Du, F., Y. Q. Lu, et al. "Electrically tunable liquid-crystal photonic crystal fiber," *Appl. Phys. Lett.*, Vol. 85, 2181, 2004.
32. Mendoza-Suarez, A., H. Perez-Aguilar, and F. Villa-Villa, "Optical response of a perfect conductor waveguide that behaves as a photonic crystal," *Progress In Electromagnetics Research*, Vol. 121, 433, 2011.
33. Erickson, D., T. Rockwood, T. Emery, A. Scherer, and D. Psaltis, "Nanofluidic tuning of photonic crystal circuits," *Optics Letters*, Vol. 31, 59–61, 2006.
34. Intonti, F., S. Vignolini, V. Turck, M. Colocci, B. L. Pavesi, S. L. Schweizer, R. Wehrspohn, and D. Wiersma, "Rewritable photonic circuits," *Appl. Phys. Lett.*, Vol. 89, 2111171–2111173, 2006.
35. Smith, C. L. C., D. K. C. Wu, M. W. Lee, C. Monat, S. Tomljenovic-Hanic, C. Grillet, B. J. Eggleton, D, Freeman, Y. Ruan, S. Madden, B. Luther-Davies, H. Giessen, and Y. H. Lee, "Microfluidic photonic crystal double heterostructures," *Appl. Phys. Lett.*, Vol. 91, 1–3, 121103, 2007.